

# One-Dimensional Spin Chains from Cu<sup>II</sup> Ions and 2,5-Bis(pyrazol-1-yl)-1,4-dihydroxybenzene

Robert Dinnebier<sup>a,\*</sup>, Hans-Wolfram Lerner<sup>b</sup>, Li Ding<sup>b</sup>, Kenneth Shankland<sup>c</sup>, William I. F. David<sup>c</sup>, Peter W. Stephens<sup>d</sup>, and Matthias Wagner<sup>b,\*</sup>

<sup>a</sup> Stuttgart, Max-Planck Institute for Solid State Research

<sup>b</sup> Frankfurt(Main), Department of Inorganic Chemistry, J. W. Goethe University

<sup>c</sup> Chilton, Didcot, Oxon/ UK, ISIS Facility, Rutherford Appleton Laboratory

<sup>d</sup> Stony Brook, N.Y./U.S.A., Department of Physics and Astronomy, SUNY at Stony Brook

Received January 19th, 2001, revised July 8th 2001.

**Abstract.** The purple colored coordination polymer [1Cu]<sub>n</sub> was obtained from 2,5-bis(pyrazol-1-yl)-1,4-dihydroxybenzene and CuBr<sub>2</sub> in aqueous ammonia. The crystal structure of [1Cu]<sub>n</sub> was determined from high resolution X-ray powder diffraction data using the method of simulated annealing. In the solid state, [1Cu]<sub>n</sub> features largely independent linear chains, all of them being oriented parallel to the *c*-axis of the crystal. The Cu ions are coordinated in a square-pla-

nar fashion by two nitrogen atoms and two anionic oxygen donors. Magnetic susceptibility and magnetization measurements indicate the Cu ions in [1Cu]<sub>n</sub> to be antiferromagnetically coupled with a coupling constant of about 20 K.

**Keywords:** Powder diffraction; Simulated annealing; One-dimensional spin chain; Copper coordination polymer

## Eindimensionale Spin-Ketten aus Cu<sup>II</sup> Ionen und 2,5-Bis(pyrazol-1-yl)-1,4-dihydroxybenzen

**Inhaltsübersicht.** Das violett gefärbte Koordinationspolymer [1Cu]<sub>n</sub> wurde aus 2,5-bis(pyrazol-1-yl)-1,4-dihydroxybenzen und CuBr<sub>2</sub> in wässrigem Ammoniak erhalten. Die Kristallstruktur von [1Cu]<sub>n</sub> wurde aus hochaufgelösten Röntgen-Pulverbeugungsaufnahmen mittels der Methode des „Simulated Annealing“ bestimmt. Im Festkörper zeigt [1Cu]<sub>n</sub> weitgehend unabhängige lineare Ketten, die allesamt paral-

lel zur kristallographischen *c*-Achse ausgerichtet sind. Die Cu-Ionen sind quadratisch planar von zwei Stickstoff-Atomen und zwei anionischen Sauerstoff-Donatoren umgeben. Magnetische Suszeptibilitäts- und Magnetisierungsmessungen belegen, dass die Cu-Ionen in [1Cu]<sub>n</sub> mit einer Kopplungskonstante von etwa 20 K antiferromagnetisch gekoppelt sind.

### Introduction

Oligonuclear complexes featuring paramagnetic transition metal ions are of great importance for the development of new molecule-based magnets and electronic materials [1–7]. Metal-containing chain compounds, which occupy an intermediate situation between clusters of high nuclearity and three-dimensional extended lattices, are of special interest, since the physics of one-dimensional magnetic materials has long been and still is an area of vivid research.

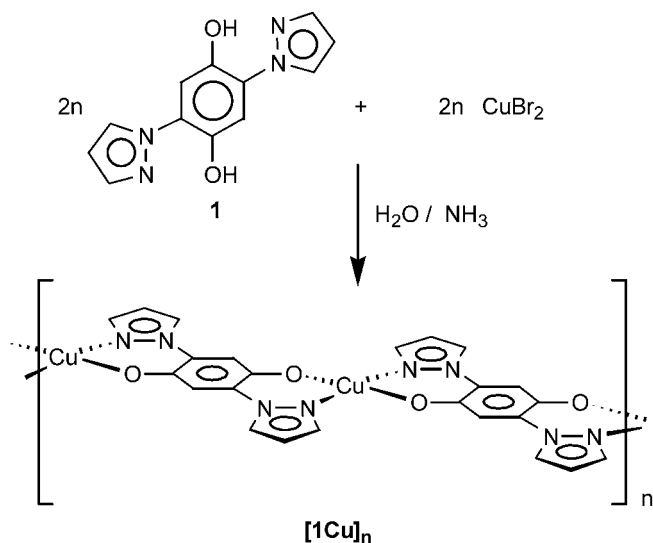
One particularly simple spin chain is provided by an array of equally spaced copper(II) ions with  $S_{\text{Cu}} = 1/2$  local spins. A great advantage of Cu<sup>II</sup> lies in the fact, that a square planar coordination sphere is preferred over an octahedral one, which minimizes

the chance of unwanted interchain crosslink formation. To bring about electronic and magnetic interactions between individual metal centers, bridging ligands possessing a rigid  $\pi$ -conjugated framework have shown to be well-suited [7]. Among those, quinoid linkers are particularly attractive, because their redox activity is preserved after they have been attached to the metal ions. Quinone, semiquinone or hydroquinone bridges can thus be established, which tend to differ in their molecular structures as well as in their metal-ligand orbital interactions. For these reasons, ligand **1** [8, 9], built from a hydroquinone core and two chelating nitrogen anchor groups, appears to be a promising bridging unit for the generation of polymeric metal-containing materials (Scheme 1).

Dinuclear transition metal (e.g. Rh, Ir, Ru, Os) complexes of **1** have already been described in the literature [10–13]. Here we report on the synthesis of the coordination polymer [1Cu]<sub>n</sub> (Scheme 1), its crystal structure determination from high resolution X-ray powder diffraction data and some preliminary magnetic measurements.

\* Dr. R. Dinnebier

Max-Planck Institute for Solid State Research  
Heisenbergstrasse 1  
D-70569 Stuttgart, Germany  
E-mail: r.dinnebier@fkf.mpg.de



**Scheme 1** Synthesis of  $[1\text{Cu}]_n$ .

## Results and Discussion

### Synthesis of $[1\text{Cu}]_n$

Purple microcrystalline  $[1\text{Cu}]_n$  was obtained by layering a solution of 2,5-bis(pyrazol-1-yl)-1,4-dihydroxybenzene in  $\text{CH}_2\text{Cl}_2$  with a solution of  $\text{CuBr}_2$  in concentrated aqueous ammonia.

### Magnetic measurements on $[1\text{Cu}]_n$

Magnetic susceptibility measurements as a function of temperature,  $\chi(T)$ , employing a SQUID-magnetometer reveal a broad maximum at around 13 K followed by a low temperature upturn. The latter becomes significantly reduced in external fields up to 5 T. So the field dependence of the magnetic susceptibility can be explained by saturation of paramagnetic  $S = 1/2$  impurities in the spin system. They can be caused by configurational inhomogeneities in the magnetic coupling strength or by finite size effects. These results are confirmed by high field ESR-experiments above 10 T.

The  $\chi(T)$  maximum around  $T_{\text{max}} \approx 13$  K is consistent with the behaviour expected for a quasi one-dimensional antiferromagnetic spin system ( $J < 0$ ) with a

**Table 1** Selected bond lengths/Å, angles/°, and torsion angles/° of  $[1\text{Cu}]_n$ . Realistic standard deviations according to ref. [25] are given

Cu–Cu (intrachain, along <i>c</i> -axis)	8.226(1)
Cu–Cu (interchain, stack along <i>a</i> -axis)	5.169(1)
Cu–Cu (interchain, neighboring stacks along <i>b</i> -axis)	7.961(1)
Cu–O(2)	1.8(1)
Cu–N(6)	2.0(1)
H–H (interchain)	1.9(1)
O(2)–Cu–N(6)	83(1), 97(1)
C(3)–C(4)–N(5)–N(6)	24(1)

nearest neighbor coupling constant of  $|J| = k_B \cdot T_{\text{max}} / 0.641$ . For the coupling constant  $J$  we obtained a value of  $|J|/k_B \approx 20$  K from our experimental data. For the analysis we use a spin Hamiltonian of the form:  $H = -J\sum_{[i,j]} S_i \cdot S_j$ . More details on the magnetic properties of  $[1\text{Cu}]_n$  including the numerical analysis will be given elsewhere (ref. [14]).

In fact, judging from the crystal structure as will be discussed below, the dominant exchange path is along the polymeric chains via Cu–ligand–Cu interaction. On the other hand, due to the Cu–Cu distance of about 5.2 Å (see table 1) perpendicular to the chains, a substantially weaker interchain interaction is expected.

### X-ray crystal structure determination of $[1\text{Cu}]_n$

In the solid state,  $[1\text{Cu}]_n$  forms independent one-dimensional polymeric chains consisting of deprotonated 2,5-bis(pyrazol-1-yl)-1,4-dihydroxybenzene molecules, bridged by Cu<sup>II</sup> cations. All chain axes are oriented along the *c*-direction of the crystal, running through the copper ions at  $1/2, 1/2, 1/2$  and the center of the six-membered ring at  $1/2, 1/2, 0$ , which are both situated on centers of symmetry in space group  $P\bar{1}$ . The Cu<sup>II</sup> ions are coordinated in an almost square planar fashion by two pyrazolyl nitrogen atoms and two oxygen atoms of the deprotonated dihydroxybenzene groups (*trans* configuration; Fig. 1). The chains are arranged in stacks along the *a*-axis of the crystal. The shortest Cu–Cu distance between the chains within each stack possesses a value of 5.2 Å (Fig. 2). All other distances between copper ions, intrachain as well as interchain distances between neighboring stacks, are greater than 8 Å. The closest contact between hydrogen atoms of neighboring chains amounts to 1.89 Å. The pyrazolyl rings within the stacks are parallel to each other and tilted by approx. 65° against the *bc*-face of the unit cell. Due to the low crystallinity and the resulting low quality powder pattern of  $[1\text{Cu}]_n$ , it was neither possible to refine individual atomic positions nor individual bond lengths. We have, however, been able to determine the position, orientation and the torsion angles of the idealised deprotonated 2,5-bis(pyrazol-1-yl)-1,4-dihydroxybenzene molecule as well as the position of the copper ion with reasonable accuracy. Difference Fourier maps show small peaks with a maximum density of 1 electron/Å<sup>3</sup> in a distance of approximately 1.2 Å above and below the coordination plane of the copper ions. This might either be an artifact or indicates a slight disorder of the copper ions. Moreover, the presence of a small amount of coordinating solvent (e.g. water or ammonia molecules), although unlikely, cannot be entirely excluded. A list of relevant bond lengths, bond angles and torsion angles is given in Tab. 1.

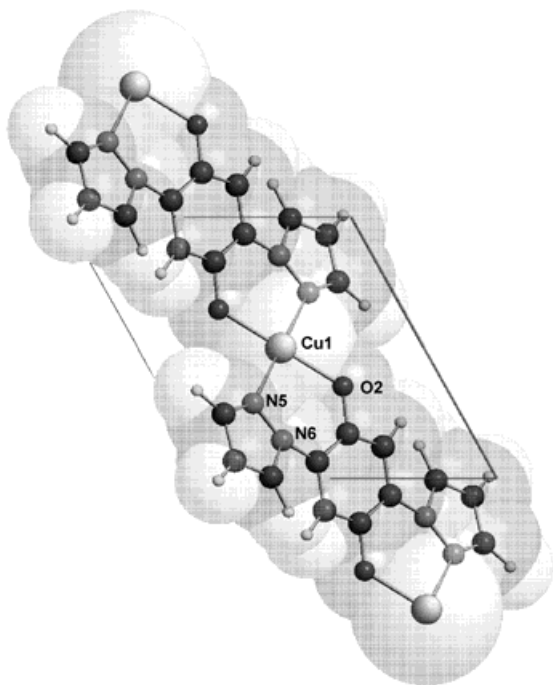


**Fig. 1** Crystal structure of  $[1\text{Cu}]_n$ . Space filling model showing the polymeric nature of the compound in a projection along the  $a$ -axis.

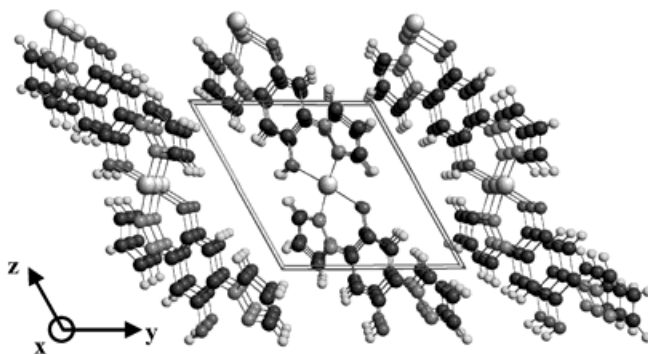


**Fig. 2** Crystal structure of  $[1\text{Cu}]_n$ . Perspective view of the packing of the molecules in a projection along the  $a$ -axis.

## Conclusion

$\text{Cu}^{\text{II}}$  ions bridged by O,N-coordination to deprotonated 2,5-bis(pyrazol-1-yl)-1,4-dihydroxybenzene moieties were found to form linear spin chains with antiferromagnetically coupled paramagnetic centers. The organic linker, which is readily accessible, can be derivatized in numerous ways (e.g. introduction of donor/acceptor substituents into the 3 and 6 positions of the hydroquinone core, generation of isomeric structures). Work is currently in progress to investigate the effect of these derivatizations on the degree of spin-spin coupling in the respective coordination polymers. Structure determination of molecular com-

pounds from powder diffraction data by means of global optimization methods in direct space like the method of simulated annealing is becoming routine and it can be shown that even in case of low quality powder diffraction data, it is nowadays possible to derive the crystal packing, which is the key information to understand the properties of the material.

## Experimental Section

**1** was synthesized according to the literature [8, 9].

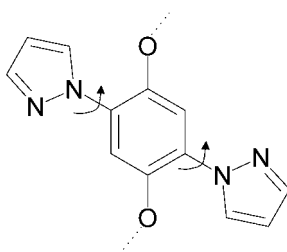
**Synthesis of  $[1\text{Cu}]_n$ :** A solution of 2,5-bis(pyrazol-1-yl)-1,4-dihydroxybenzene **1** (0.066 g, 0.272 mmol) in 10 mL of  $\text{CH}_2\text{Cl}_2$  was layered with a solution of  $\text{CuBr}_2$  (0.179 g, 0.803 mmol) in 5 mL of concentrated aqueous ammonia. A purple microcrystalline material formed after one week. The liquid was removed by filtration. The remaining product was triturated with  $\text{H}_2\text{O}$  ( $3 \times 5$  mL),  $\text{CH}_2\text{Cl}_2$  ( $3 \times 5$  mL) and dried in air. Yield: 0.079 g (95%).

**Crystal structure determination of  $[1\text{Cu}]_n$ :** X-ray powder diffraction data were collected at 295 K on beamline X3B1 of the Brookhaven National Synchrotron Light Source ( $\lambda = 1.14991(2)$  Å) in transmission geometry with the sample sealed in a 0.7 mm lithiumborate glass (No. 50) capillary (Tab. 2). Data reduction was performed using the GUF1 [15] program. Indexing with ITO [16] led to a primitive triclinic unit cell with lattice parameters given in Tab. 2. The number of formula units per unit cell could be determined to  $Z = 1$  from packing considerations, indicating  $P\bar{1}$  as the most probable space group, which could later be confirmed by Rietveld refinement. The peak profiles and precise lattice parameters were determined by LeBail-type fits using the program Fullprof [17]. The background was modeled manually using GUF1. The peak-profile was described by a pseudo-Voigt function in combination with a special function that accounts for the asymmetry due to axial divergence [18].

The crystal structure was solved using the DASH [19] structure solution package as follows: Data in the range  $5^\circ \leq 2\theta \leq 40.5^\circ$  were subjected to a Pawley refinement [20] in space group  $P1$  in order to extract 129 correlated integrated intensities from the pattern. A good fit to the data ( $\chi^2 = 1.54$ ) was obtained. An internal coordinate description of the organic moiety (Fig. 3) was constructed using standard bond lengths, angles and torsion angles. Those torsion angles that could not be assigned precise values in advance were flagged as variables for refinement in the simulated annealing procedure. Since the presence of an inversion center was not known *a priori*, a decision was taken to solve the structure in  $P1$  with two independent unknown torsion angles present within the structure (Fig. 3). The position, orientation and conformation of the organic moiety in the refined unit cell were postulated whilst the position of the Cu atom was held fixed at  $1/2, 1/2, 1/2$  and the level of agreement between the trial structure and the experimental diffraction data quantified by:  $\chi^2 = \sum_h \sum_k [(I_h - c|F_h|^2)(V^{-1})_{hk}(I_k - c|F_k|^2)]$ , where  $I_h$  and  $I_k$  are Lorentz-polarisation corrected, extracted integrated intensities from the Pawley refinement of the diffraction data,  $V_{hk}$  is the covariance matrix from the Pawley refinement,  $c$  is a scale factor, and  $|F_h|$  and  $|F_k|$  are the structure factor magnitudes calculated from the trial structure. The trial structure was subjected to a global optimization

**Table 2** Crystallographic data for [1Cu]<sub>n</sub>

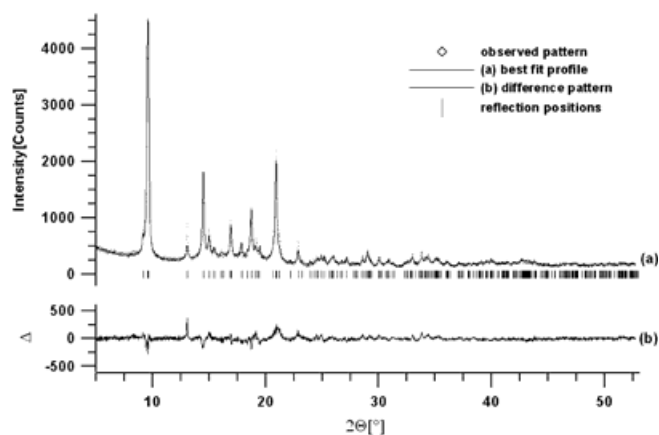
formula	CuC <sub>12</sub> N <sub>4</sub> O <sub>2</sub> H <sub>8</sub>
temperature/K	295
formula weight/(g mol <sup>-1</sup> )	303.762
space group	<i>P</i> $\bar{1}$
<i>a</i> /Å	5.1723(5)
<i>b</i> /Å	7.9587(9)
<i>c</i> /Å	8.2298(11)
$\alpha$ /°	118.221(6)
$\beta$ /°	91.520(9)
$\gamma$ /°	100.148(8)
<i>V</i> /Å <sup>3</sup>	291.47(6)
<i>Z</i>	1
calc. Density/(g cm <sup>-3</sup> )	1.731
$\mu$ /cm <sup>-1</sup> for 100% packing	66.8
$2\theta$ range/°	2.0–52.8
step size/° $2\theta$	0.02
counting time/step/sec	2.1 (2.0° ≤ $2\theta$ ≤ 40.24°)
	3.0 (30.0° ≤ $2\theta$ ≤ 52.8°)
wavelength/Å	1.14991(2)

**Fig. 3** A sketch of the 2,5-bis(pyrazol-1-yl)-1,4-dihydroxybenzene fragment with the variable torsion angles indicated by curved arrows.

[21, 22] in which torsion angles were the only internal degrees of freedom and the external degrees of freedom consisted of three fractional coordinates describing the position of the molecule and four quaternions describing its orientation. Examination of the structure giving the best fit to the data showed the organic moiety to form a polymeric structure around the Cu, with its center of mass being located very close to  $1/2, 1/2, 0$ . Accordingly, the global search was re-run with the organic moiety anchored at this point, thus reducing the problem to an orientation/conformation search. The structure giving the best fit to the data ( $\chi^2 = 7$ ) was verified by Rietveld refinement of the fractional co-ordinates obtained at the end of the simulated annealing run.

Rietveld refinements, using the GSAS program system [23], were carried out in space groups *P*1 and *P* $\bar{1}$ , establishing *P* $\bar{1}$  as the correct space group. Since unconstrained refinement resulted in severe distortions from the ideal molecular geometry, a number of soft constraints have been applied for bond lengths (weight factor of 70), the degree of planarity (weight factor of 70) and bond angles (weight factor of 30) of the 2,5-bis(pyrazol-1-yl)-1,4-dihydroxybenzene. The Rietveld refinement converged quickly to the R-values given in the caption of Fig. 4.

It should be noted that the powder pattern of [1Cu]<sub>n</sub> exhibits severe anisotropic peak broadening caused by lattice strain with the sharpest peaks along [100] direction (parallel to the Cu–Cu vector of consecutive polymer chains), which could be described to a satisfactory degree by the uniaxial strain model in GSAS.

**Fig. 4** Scattered X-ray intensity for [1Cu]<sub>n</sub> at ambient temperature as a function of the diffraction angle  $2\theta$ . Shown are the observed pattern (diamonds), the best Rietveld fit profile (line), the reflection positions and the difference trace at the bottom. The wavelength was  $\lambda = 1.14991(2)$  Å. The R-values are R-p = 8.2%, R-wp = 10.6%. R-p and R-wp refer to the Rietveld criteria of fit for profile and weighted profile, respectively, defined in ref. [24].**Table 3** Positional parameters,  $U_i/U_e \cdot 10^2$  of [1Cu]<sub>n</sub> in *P* $\bar{1}$  symmetry at 295 K from the simulated annealing run using rigid bodies. The estimated standard deviations and the temperature factors and were taken from the Rietveld refinement, the latter are constrained to be equal within the 2,5-bis(pyrazol-1-yl)-1,4-dihydroxybenzene molecule. Due to the limited accuracy of powder diffraction data, the given esd's of the Rietveld refinement according to ref. [25] should be multiplied by at least a factor of 6

	<i>x</i> / <i>a</i>	<i>y</i> / <i>b</i>	<i>z</i> / <i>c</i>	$U_i/U_e \times 10^2$
Cu1	0.5	0.5	0.5	8.7(5)
O2	0.4639(3)	0.3582(3)	-0.3809(2)	3.4(5)
C3	0.4745(2)	0.4248(3)	-0.2025(2)	3.4(5)
C4	0.6702(2)	0.5825(2)	-0.0783(2)	3.4(5)
N5	0.8462(2)	0.6693(2)	-0.1395(3)	3.4(5)
N6	0.8050(4)	0.6631(3)	-0.2999(2)	3.4(5)
C7	1.0268(4)	0.7687(4)	-0.3173(3)	3.4(5)
C8	1.2079(3)	0.8401(3)	-0.1599(4)	3.4(5)
C9	1.0868(4)	0.7735(4)	-0.0487(3)	3.4(5)
H10	1.1590	0.7966	0.0693	3.4(5)
H11	1.3803	0.9189	-0.1345	3.4(5)
H12	1.0542	0.7903	-0.4201	3.4(5)
C13	0.6873	0.6536	0.1127	3.4(5)
H14	0.8256	0.7602	0.1939	3.4(5)

It should further be noted that the quality of the powder pattern is very low with a peak to background ratio of  $\leq 12:1$  and a FWHM of the sharpest peak of  $0.07^\circ 2\theta$  in [100] direction and almost twice that value for other directions. Restrained refinement of the atomic positions resulted in slightly improved fits but some unreasonable distances between hydrogen atoms at calculated positions occurred. Therefore, the rigid body coordinates from the simulated annealing run and the isotropic temperature factors of the Rietveld refinement are given in Table 3.

**Acknowledgement.** Research was carried out in part at the National Synchrotron Light Source at Brookhaven National

Laboratory, which is supported by the US Department of Energy, Division of Materials Sciences and Division of Chemical Sciences. The SUNY X3 beamline at NSLS is supported by the Division of Basic Energy Sciences of the US Department of Energy under Grant No. DE-FG02-86ER45231. P. W. S. was partially supported by the National Science Foundation under grant DMR-95-01325. Financial support by the Deutsche Forschungsgemeinschaft (DFG) and the Fonds der Chemischen Industrie is acknowledged. L. D. is grateful to the Alexander von Humboldt Foundation for a postdoc grant.

## References

- [1] O. Kahn, *Acc. Chem. Res.* **2000**, *33*, 647.
- [2] P. Nguyen, P. Gómez-Elipé, I. Manners, *Chem. Rev.* **1999**, *99*, 1515.
- [3] I. Cuadrado, M. Morán, C. M. Casado, B. Alonso, J. Lozada, *Coord. Chem. Rev.* **1999**, *193–195*, 395.
- [4] B. Jiang, S. W. Yang, S. L. Bailey, L. G. Hermans, R. A. Niver, M. A. Bolcar, W. E. Jones, Jr., *Coord. Chem. Rev.* **1998**, *171*, 365.
- [5] R. J. Mortimer, *Chem. Soc. Rev.* **1997**, *26*, 147.
- [6] C. U. Pittman, Jr., C. E. Carraher, Jr., M. Zeldin, J. E. Sheats, B. M. Culbertson (Eds.), *Metal-Containing Polymeric Materials*, Plenum Press 1996.
- [7] O. Kahn, *Molecular Magnetism*, Wiley-VCH 1993.
- [8] W. Gauß, H. Heitzer, S. Petersen, *Liebigs Ann. Chem.* **1972**, *764*, 131.
- [9] J. Catalán, F. Fabero, M. S. Guijarro, R. M. Claramunt, M. D. Santa Maria, M. d. I. C. Foces-Foces, F. H. Cano, J. Elguero, R. Sastre, *J. Am. Chem. Soc.* **1990**, *112*, 747.
- [10] A. M. Bond, F. Marken, C. T. Williams, D. A. Beattie, T. E. Keyes, R. J. Forster, J. G. Vos, *J. Phys. Chem. B* **2000**, *104*, 1977.
- [11] T. E. Keyes, R. J. Forster, P. M. Jayaweera, C. G. Coates, J. J. McGarvey, J. G. Vos, *Inorg. Chem.* **1998**, *37*, 5925.
- [12] T. E. Keyes, P. M. Jayaweera, J. J. McGarvey, J. G. Vos, *J. Chem. Soc., Dalton Trans.* **1997**, 1627.
- [13] P. Cornago, C. Escolástico, M. D. Santa Maria, R. M. Claramunt, D. Carmona, M. Esteban, L. A. Oro, C. Foces-Foces, A. L. Llamas-Saiz, J. Elguero, *J. Organomet. Chem.* **1994**, *467*, 293.
- [14] S. Zherlitsyn, B. Wolf, C. D. Bredl, M. Lang, B. Lüthi, *manuscript in preparation*.
- [15] R. E. Dinnebier, L. W. Finger, *Z. Krist. Suppl.* **1998**, *15*, 148; available through <http://www.pulverdiffraktometrie.de>.
- [16] J. W. Visser, *J. Appl. Cryst.* **1969**, *2*, 89.
- [17] J. Rodríguez-Carvajal, *Abstracts of the Satellite Meeting on Powder Diffraction of the XV Congress of the IUCr*, Toulouse, France 1990, 127.
- [18] L. W. Finger, D. E. Cox, A. P. Jephcoat, *J. Appl. Cryst.* **1994**, *27*, 892.
- [19] DASH is a product of Cambridge Crystallographic Data Centre, 12, Union Road, Cambridge, CB2 1EZ, UK.
- [20] G. S. Pawley, *J. Appl. Cryst.* **1981**, *14*, 357.
- [21] W. I. F. David, K. Shankland, N. Shankland, *Chem. Commun.* **1998**, 931.
- [22] R. E. Dinnebier, M. Wagner, F. Peters, K. Shankland, W. I. F. David, *Z. Anorg. Allg. Chem.* **2000**, *626*, 1400.
- [23] A. C. Larson, R. B. Von Dreele, *GSAS – General Structure Analysis System*, Los Alamos National Laboratory Report LAUR 86–748 1994, available by anonymous FTP from [mist.lansce.lanl.gov](mailto:mist.lansce.lanl.gov).
- [24] I. Langford, D. Louër, *Rep. Prog. Physics.* **1996**, *59*, 131.
- [25] R. J. Hill, L. M. D. Cranswick, *J. Appl. Cryst.* **1994**, *27*, 802.